Zeolite Structure Direction: Identification, Strength and Involvement of Weak CH···O Hydrogen Bonds

Tzonka Mineva, Eddy Dib, Arnold Gaje, Hugo Petitjean, Jean-louis Bantigniès, Bruno Alonso

Zeolite structure direction: identification, strength and involvement of weak CH…O hydrogen bonds

Tzonka Mineva,*[1] Eddy Dib,[1],[2] Arnold Gaje,[1] Hugo Petitjean,[1] Jean-Louis Bantignies[3] and Bruno Alonso*[1]

[1] Institut Charles Gerhardt de Montpellier, ICGM-MACS, UMR 5253 CNRS-ENSCM-UM, 240 av. du Prof. Emile Jeanbrau, 34296 Montpellier Cedex 5, France. E-mails: tzonka.mineva@enscm.fr and bruno.alonso@enscm.fr

[2] Faculty of Engineering, Polytech Beirut, Sagesse University, P.O. Box: 50-501, Beirut, Lebanon.

[3] Laboratoire Charles Coulomb, UMR 5221 CNRS-Université de Montpellier, Montpellier, France.

Abstract

We demonstrate that weak CH…O hydrogen bonds (HBs) are important host-guest interactions in zeolite assemblies involving structure directing organocations. This type of HB are identified between alkyl groups of the organic structure directing agent (OSDA) and the silica framework in as-synthesized silicalite-1 of complex topology (MFI) using a combination of experimental and theoretical data obtained at low and room temperatures. The 28 weak CH…O HB, evidenced along dynamics simulation at room temperature, represent 30% of the energy of the Coulomb electrostatic interaction between OSDA and the zeolite framework. The strongest and most stable HB found here connects the OSDA to the $[4^1 5^2 6^2]$ cage containing F atoms and should contribute to preserve zeolite topology during crystal growth. An inspection of other as-synthesized zeolites of very different framework topology indicates that the directional CH...O HBs have to be considered when discussing zeolite structure directing phenomena.

Keywords

Hydrogen bonds, Zeolites, Structure directing agent, IR spectroscopy, Density functional calculations, Ab-initio molecular dynamics

Since the first systematic investigation,[1] weak hydrogen bonds (HBs) between CH donor groups and O acceptor atoms have been evidenced and described for several organic and biological molecules.[2] Today these HBs have a recognized role in chemistry, notably in the understanding of conformational states[3] and in crystal engineering.[2c,4] In the case of the important class of oxide-based materials that are zeolites, the implication of these weak HBs in crystal formation is scarcely investigated despite their possible structure directing and stabilizing effects. For instance tetraalkylammonium cations are widely used as organic structure directing agents (OSDAs) in the hydrothermal synthesis of zeolites,[5] and are also known for a long time to form CH…X HBs with proton acceptor anions.[6] Besides, Behrens *et al*. showed the presence of HBs between the aromatic CH groups of the organometallic cobaltocenium cation $[Co(C_5H_5)_2]^+$ and the O atoms of silica in the particular case of a clathrasil framework (nonasil, NON).[7] Some years later, Hong *et al*. deducted the existence of intramolecular CH…O HBs for choline cations inside UZM-22 zeolites (MEI framework),[8] not involving directly the zeolite framework. Recently, we evidenced the possible stabilizing role of intermolecular CH…O HBs between tetramethylammonium cations and silica inside another clathrasil framework (octadecasil, AST) thanks to a combination of experimental methods (NMR, XRD) and theoretical calculations.[9]

Weak CH…O HBs are not easily identified as their individual signature can be very subtle, and often blurred in the ensemble of intermolecular interactions. In the case of OSDA-zeolite framework interactions, the difficulty is enhanced by the static and thermal disorders at the crystallographic positions. Moreover, the large number of unequivalent atoms in zeolites with complex topologies[10] still hinders the identification of CH…O H-bonding. Despite these difficulties, considering the CH…O HBs when discussing OSDA-zeolite interactions would be beneficial for the design of the final zeolite structure and properties. In this letter, we address for the first time the occurrence and characteristics of these HBs in the topologically complex MFI zeolites of high scientific and industrial interest,[5,11] by inspecting geometrical and spectroscopic (IR) data, and evaluating their strength with respect to the total OSDA-zeolite interactions, including these at finite temperature through density-functional-theory (DFT) methods and Born-Oppenheimer molecular dynamics (BOMD) simulation.

A first evidence of the presence of CH…O bonds comes through the analysis of crystal structures of as-synthesized zeolites with MFI topology containing tetrapropylammonium (TPA). In these X-ray structures, a great number of C…O distances d_{CO} are below 4.0 Å (**Supporting Information**, **Table S1**) suggesting the formation of weak HBs between H donors and O acceptors.[2c] There is also a significant number of cases where d_{CO} < 3.6 Å more certainly ascribed to HB interactions,[2b,12] notably for the TPA-F-silicalite-1 structure.[13] This zeolite synthesized in fluoride medium presents well ordered structures with a low level of chemical defects. It is chosen here to explore the existence and role of CH...O HBs.

A second experimental indication of CH…O HBs is obtained from IR spectroscopy. The variations of the CH stretching vibrations ν(CH) of the OSDA in TPA-F-silicalite-1 at 275 K and 180 K, above the orthorhombic-monoclinic phase transition,[14] are presented in **Figure 1**. They exhibit the typical ν(CH) complex pattern of this material.[15] From IR measurements as a function of the temperature (**Supporting Information**, **Figure S3**) we observe two significant gradual downshifts for ν(CH) localized at ~2850 ($\Delta\nu_{(275\text{-}180K)}$ = 4cm^{-1}) and ~2917 cm^{-1} ($\Delta\nu_{(275\text{-}180K)}$ = 2cm^{-1}) assigned respectively to symmetric and antisymmetric modes of CH_2.[16] This non classical pseudo-harmonic behavior is commonly reported when the internal stretching mode are affected by H-bonding interactions[17] meaning that at least one type of CH_x groups is involved in HBs. Furthermore, such thermal variations are observed for ν(CH) in cellulose crystals,[18] and have been recently assigned to CH…O HBs.[19]

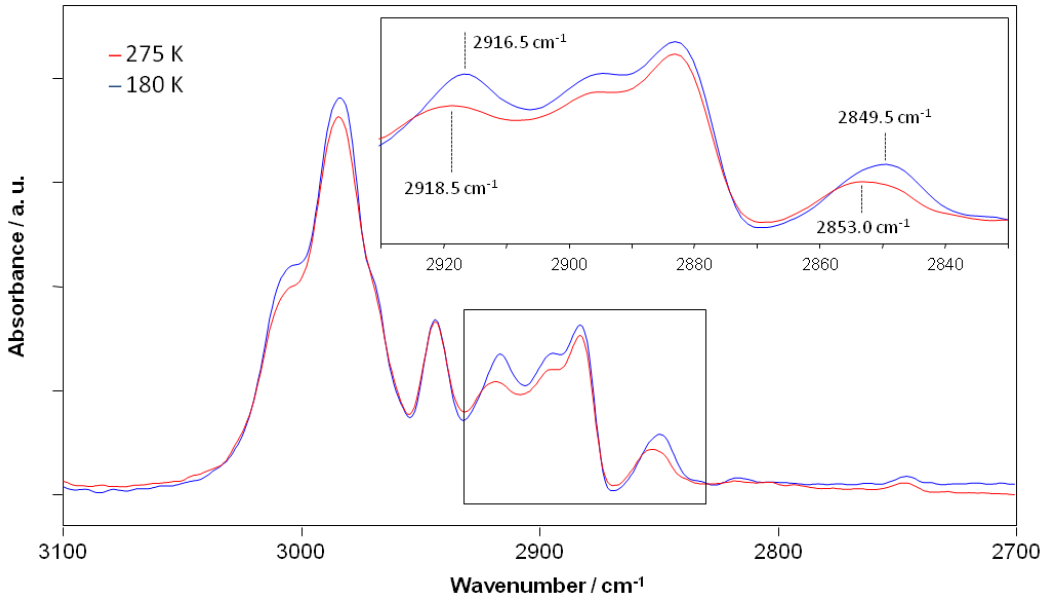

Figure 1. IR CH stretching bands of TPA-F-silicalite-1 recorded at T = 275 and 180 K.

Further information is gained from density functional theory (DFT)-based theoretical calculations and positioning of H atoms. The CHO moieties in the TPA-F-silicalite-1 crystals are analyzed in the DFT-D (D-dispersion) optimized structures (**Supporting Information**, **Table S1**). For the two space groups considered –*Pnma* the most often determined for silicalite-1 containing TPA, and $Pn2_1a$ that better accommodates the symmetry of TPA and zeolite framework – we found a great number of H…O distances d_{HO} below 3.0 Å, and a significant number (9 to 12) for which d_{HO} < 2.6 Å with CHO angles between 100 and 180°. These geometrical parameters are indeed consistent with the presence of weak HBs.[2b,20]

To circumvolve possible artifacts generated by DFT optimizations at T = 0 K, we carried out dynamics simulation (for 1.1 ps) at T = 300 K of a cluster model centered on the TPA position. The spatial organization of the silica shell and the motions experienced by TPA appear here highly compatible with the experimental crystallographic and ^{13}C and ^{14}N NMR data (**Supporting Information S6**), and importantly the TPA dynamics can be appropriately used to investigate CH…O interactions. In the resulting time-averaged cluster (**Figure 2A**), 30 d_{HO} values are falling below 3.0 Å and involve 19 H (over 28 H in TPA) and 23 O (**Supporting Information**, **Tables S1, S7a**). There is no specific cycle or cage location for the O atoms that can form one, two or three HBs although the shortest (and strongest, *vide infra*) HB is found for O in a 4 MR in the $[4^1 5^2 6^2]$ cage containing one F atom. The related 19 H atoms belong to methylene or methyl groups and can form 8 monofurcated HBs (two-center bonds with one H donor and one O acceptor) and 11 bifurcated HBs (three-center bonds with one H and two O acceptors). The histograms in **Figure 2D** presenting the number of d_{HO} values below 3.0 Å per CHO angle range after cone correction,[21] show a distinct preference for the highest angle values (170-180°). Besides, CHO angles in the time-averaged cluster tend to decrease when d_{HO} increase, while remaining above 90° (**Supporting Information**, **Figure S7a**). Such behaviors reflect the directionality of HBs (stronger when the angle is closer to 180°).[20] They confirm indeed the presence of CH…O HBs allowing to discard van der Waals interactions for these CHO moieties.[12]

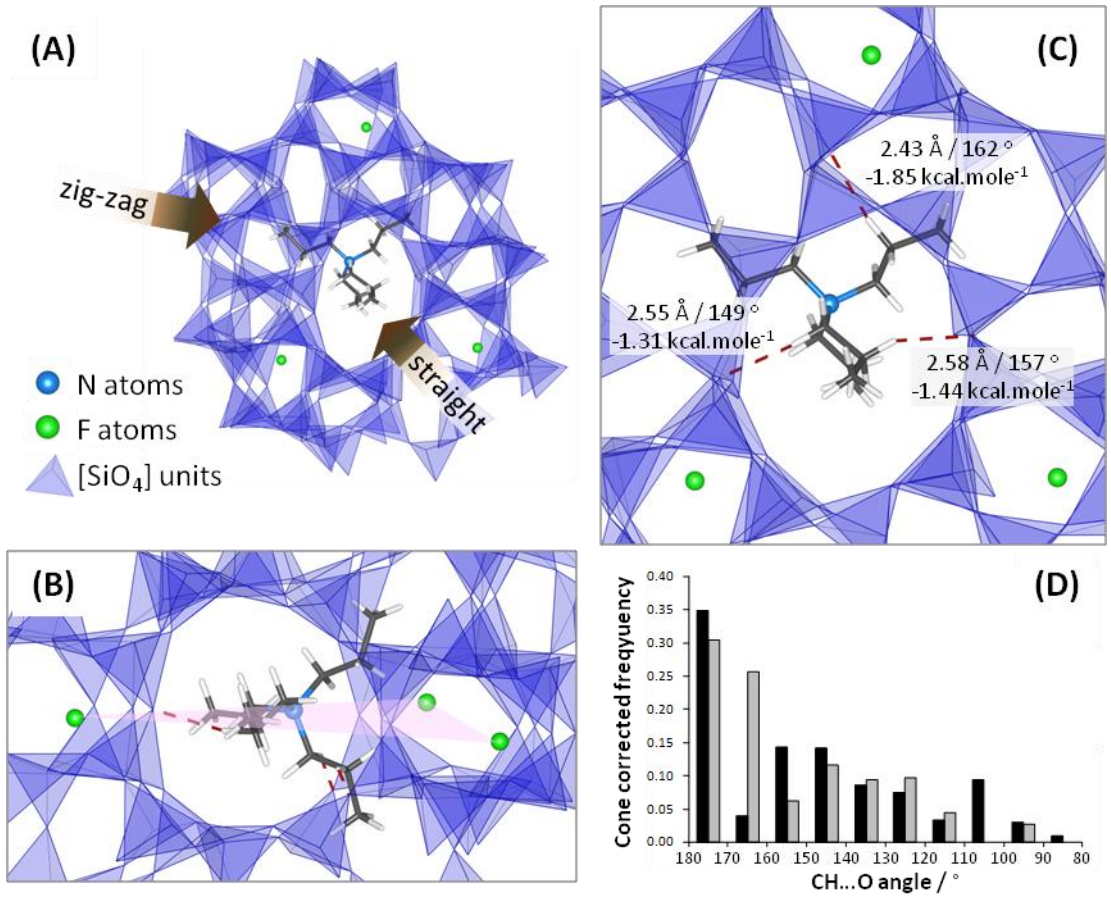

Figure 2. Time-averaged cluster: (A) general view, (B) view along zigzag channel, (C) view along the straight channel. The CH…O shortest distances are highlighted (red dashed line). The related values correspond to d_{HO},

CHO angles and HB energies. For the sake of clarity, Si, O, C and H atoms are omitted, and periphery [SiO_4] tetrahedra are removed. (D) Frequency counts histograms of CHO angles corrected by sin(CHO) for the optimized $Pn2_1a$ crystal (black columns) and the time-averaged cluster models (grey columns). Only d_{HO} < 3Å are considered.

The dynamics results are even more informative. The d_{HO} profiles as a function of the computed time allow to distinguish between: i) stable HBs (d_{HO} < 3 Å all along the dynamics), and ii) unstable HBs for which d_{HO} > 3 Å is occasionally observed (**Figure 3A**). Moreover, a sole H atom can form mono- or multi-furcated HBs with a set of different O atoms of the zeolite framework (**Figure 3B**). This reflects a competition between thermally activated alkyl group motions and attractive CH…O interactions. The particular location of the H atoms with respect to the MFI silica framework would then determine the stability and strength of the HB (*vide infra*).

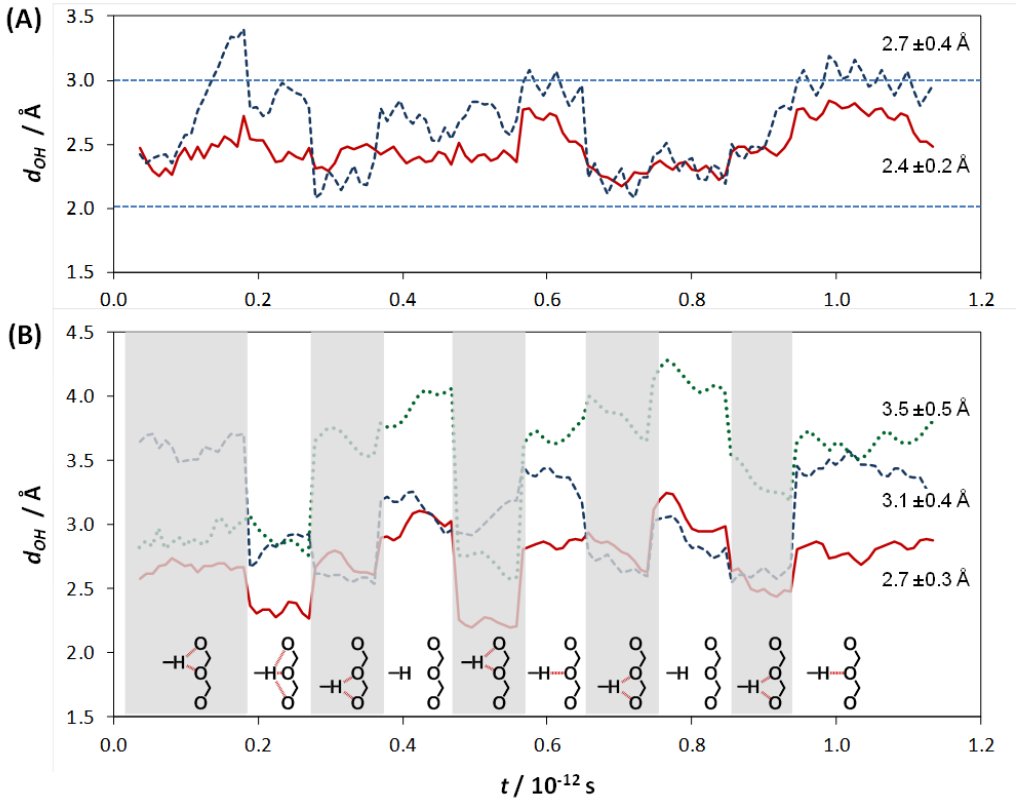

Figure 3. Variations of d_{HO} distances along the BOMD simulations for: (A) two different H and O pairs, (B) one H with three different O. For this latter case, the schemes under the curves represent the type (mono-, bi-, tri-furcated or no H-bond) of H-bond interactions occurring at each time interval.

Besides these geometrical and spectroscopic aspects, it is noteworthy that the covalent CH bond is polarized as deduced from the atomic partial charges (with Mulliken scheme, see **Supporting Information**, **Tables S8**), an additional criterion for the formation of HBs.[22] H atoms are positively charged on the contrary to N and C, and the differences in partial charges between H and negatively

charged O are close to +0.8 confirming that the electrostatic interaction drive the CH...O bond formation.[2b,20] Therefore the OSDA-zeolite electrostatic interactions depend predominantly on the attractive interaction between H and O atoms at the organic-inorganic interface.

In the typical electron density maps of the time-averaged cluster model (**Figure 4**), a residual density of ca. 0.02 e^- is found between H and O atoms forming HBs. This electron density explains the decrease in the global charge of TPA in interaction with the silica framework (+0.86) below its nominal charge +1. This feature, noticed previously for octadecasil and ZSM-5 zeolites containing OSDA,[9,23] suggests therefore a local stabilization of the system by charge transfers between the organic and the inorganic moieties through H-bonding. Furthermore, the three shortest and strongest CH...O bonds are spatially close to F and N, and to the plane containing these atoms (**Figure 2B**). Seen along the normal axis of this plane, corresponding to the (0*k*0) planes in the crystal, the projections of the three HBs are located inside the triangle formed by the F atoms, each of them being between one N and one F atom (**Figure 2C**). This particular location appears consistent with a maximization of the electrostatic interaction between the positive charge brought by TPA and the negative charges brought by fluoride anions during the synthesis. From the potential energy density calculated at the characteristic HB critical points (3, -1),[22] the energy of the HB per O (E^{HB}) is estimated[24] to -1.85 kcal.mole^{-1} for the monofurcated bond in **Figure 4A**. This HB is the strongest, the shortest (2.43 Å, **Figure 2C**) and the most stable found by dynamics simulation (**Figure 3A**), and therefore one of the most able to preserve the zeolite topology during crystal growth. Its specific position, connecting a CH_2 group of TPA to the 4 MR of the $[4^15^26^2]$ cage containing F, can be understood in that sense. The relative position of this CH_2 and the $[4^15^26^2]$ cage is also found in optimized and non-optimized crystal structures with $2.9 < d_{CO} < 3.7$ Å (**Supporting Information**, **Table S7b**). For the other HBs E^{HB} values are between -1.44 and -0.62 kcal.mole^{-1}, a typical range for weak CH…O HBs.[2b] In line with earlier H-bonding studies,[24] E^{HB} follows an exponential law against d_{HO} for the 28 shortest d_{HO} that can be considered as real HBs (**Supporting Information**, **Figure S7b**). The sum of these 28 E^{HB} values is -27 kcal.mol^{-1}. This energy is comparable to that calculated for the dispersion interaction of OSDA with zeolite framework (-39 kcal.mol^{-1}) and represents 30% of the Coulomb interaction energy (-92 kcal.mol^{-1}).

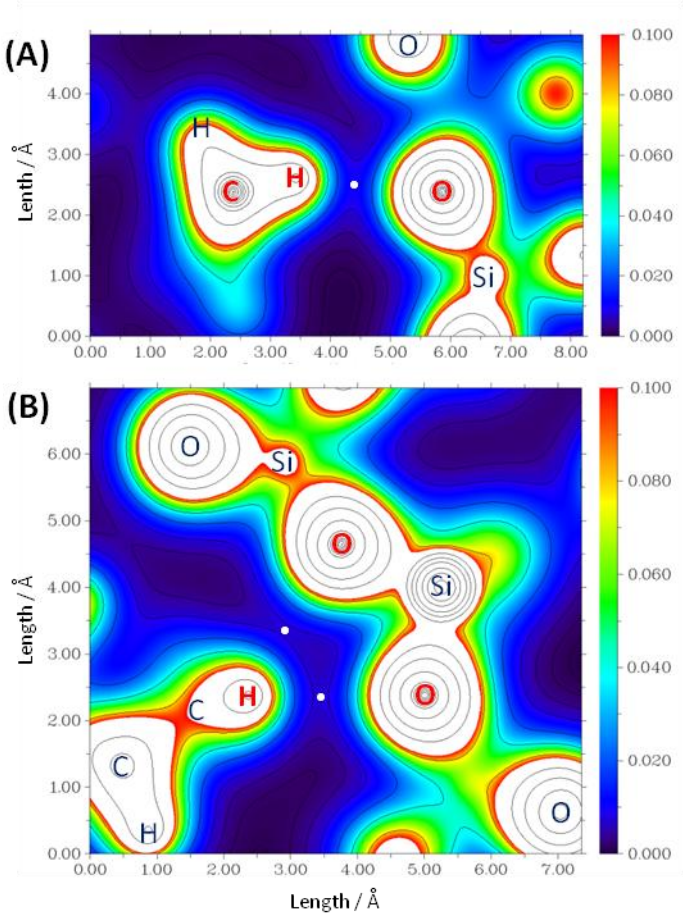

Figure 4. Electron density maps of the time-averaged cluster: (A) monofurcated HB (plotted in CHO plane); (B) bifurcated HB (plotted in HOO plane). Red and blue labels correspond to atoms in plane and slightly out of plane respectively. White dots represent the critical (3,-1) points between H and O.

In this study we have thoroughly investigated CH...O HBs in TPA-F-silicalite-1 zeolites; however short C-O distances (< 4 Å) also exist in other, very different, as-synthesized zeolites. Strikingly the normalized d_{CO} frequency counts distributions (**Figure 5**) appeared rather similar for a series of as-synthesized silica zeolites of contrasted topological complexity,[10] and obtained in fluoride media using organoammonium cations with different C/N ratio. This similarity can be rationalized by the favored formation of CH…O HBs, indicating that HB interactions have a widespread role in zeolite formation.

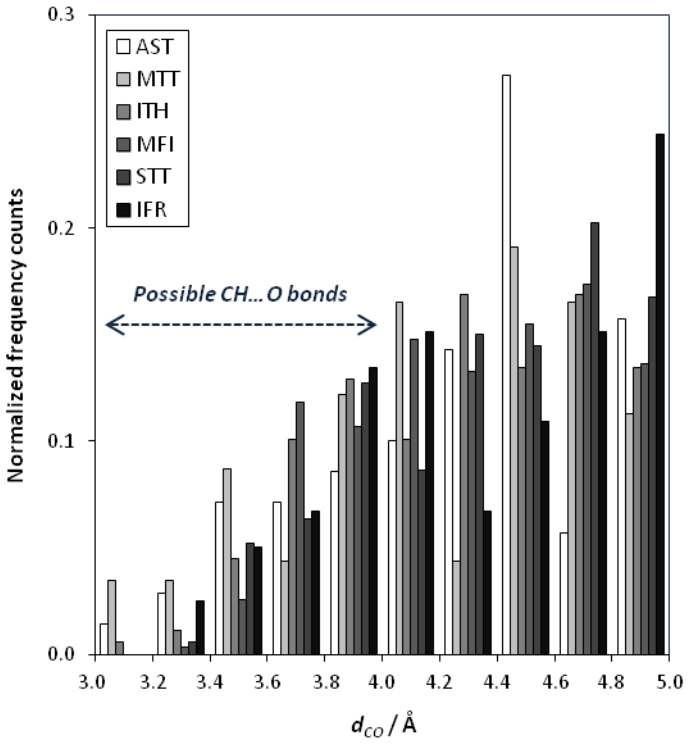

Figure 5. Normalized frequency counts histograms of d_{CO} distances below 5 Å retrieved from crystal structures of a series of as-synthesized zeolites. All zeolites have a silica framework and are obtained through fluoride routes. Their differences lye in the topology (see legend) and the OSDA: tetramethylammonium (C/N = 4) for AST octadecasil,[25] N,N′-diisopropylimidazolium (C/N = 4.5) for MTT,[26] hexamethonium cations (diquat, C/N = 6) for ITH-ITQ13,[27] TPA (C/N = 12) for MFI silicalite-1,[13] N,N,N-trimethyl-1-adamantammonium (C/N = 13) for STT-SSZ-23,[28] and N-benzylquinuclidinium (C/N = 14) for IFR-ITQ4.[29]

OSDA-zeolite host-guest interactions are known to be governed at least by van der Waals and electrostatic interactions leading to close contacts between organic groups and the oxide network.[30] In spite of that, the existence and directional role of CH…O HBs have been largely neglected until now. Thanks to experimental data and DFT/BOMD calculations at different temperatures, we demonstrate here the ubiquitous presence of stable and dynamically unstable weak CH…O bonds in as-synthesized complex MFI zeolites, and highlighted their stabilizing role in OSDA-zeolite interactions. The identification and fine characterization of these interactions in other OSDA-zeolite framework associations would bring essential information on directing effects in zeolites. Understanding the strength and directionality of the CH…O HBs can therefore be of paramount importance for the design of the final zeolite structure and properties, such as acid site distribution and chirality.

Acknowledgements

The authors thank the IRAMAN platform of the University of Montpellier for providing access to IR facility and computational resources, grant ID: A0050807369 by GENCI.

Table of Contents

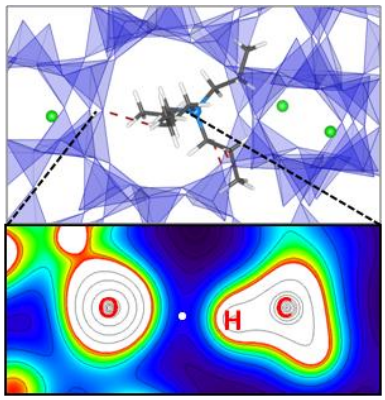

Weak CH…O hydrogen bonds between organic structure directing agents and silica framework are important host-guest interactions as demonstrated for silicalite-1 (complex topology MFI). These directional intermolecular interactions need also to be considered for various other zeolites in addition to van der Waals and Coulomb interactions.

References

[1] D. J. Sutor, *Nature* **1962**, *195*, 68-69.

[2] a) R. Taylor, O. Kennard, *J. Am. Chem. Soc.* **1982**, *104*, 5063-5070; b) T. Steiner, *Crystallog. Rev.* **2003**, *9*, 177-228; c) G. R. Desiraju, *Chem. Comm.* **2005**, 2995-3001.

[3] a) O. Takahashi, Y. Kohno, M. Nishio, *Chem. Rev.* **2010**, *110*, 6049–6076; b) C. R. Jones, P. K. Baruah, A. L. Thompson, S. Scheiner, M. D. Smith, *J. Am. Chem. Soc.* **2012**, *134*, 12064-12071.

[4] a) K. Biradha, *CrystEngComm* **2003**, *5*, 374-384; b) R. Taylor, *Cryst. Growth Des.* **2016**, *16*, 4165-4168.

[5] C. S. Cundy, P. A. Cox, *Chem. Rev.* **2003**, *103*, 663-701.

[6] K. M. Harmon, I. Gennick, S. L. Madeira, *J. Phys. Chem.* **1974**, *78*, 2585-2591.

[7] P. Behrens, G. van de Goor, C. C. Freyhardt, *Angew. Chem. Int. Ed.* **1996**, *34*, 2680-2682.

[8] M. B. Park, S. J. Cho, S. B. Hong, *J. Am. Chem. Soc.* **2011**, *133*, 1917-1934.

[9] E. Dib, M. Freire, V. Pralong, T. Mineva, B. Alonso, *Acta Cryst. C* **2017**, *73*, 202-207.

[10] S. V. Krivovichev, *Microporous Mesoporous Mater.* **2013**, *171*, 223-229.

[11] W. Vermeiren, J. P. Gilson, *Top. Catal.* **2009**, *52*, 1131-1161.

[12] T. Steiner, G. R. Desiraju, *Chem. Commun.* **1998**, 891-892.

[13] E. Aubert, F. Porcher, M. Souhassou, V. Petricek, C. Lecomte, *J. Phys. Chem. B* **2002**, *106*, 1110-1117.

[14] J. M. Chezeau, L. Delmotte, T. Hasebe, N. B. Chanh, *Zeolites* **1991**, *11*, 729-731.

[15] M. Nowotny, J. A. Lercher, H. Kessler, *Zeolites* **1991**, *11*, 454-459.

[16] G. Socrates, *Infrared and Raman characteristic group frequencies: tables and charts*, 3rd ed., John Wiley and sons, Chichester, **2001**.

[17] J. L. Bantignies, L. Vellutini, J. L. Sauvajol, D. Maurin, M. WongChiMan, P. Dieudonné, J. J. E. Moreau, *J. Non-Cryst. Solids* **2004**, *345*, 605-609.

[18] S. Kokot, B. Czarnik- Matusewicz, Y. Ozaki, *Biopolymers* **2002**, *67*, 456-469.

[19] C. M. Altaner, Y. Horikawa, J. Sugiyama, M. C. Jarvis, *Cellulose* **2014**, *21*, 3171-3179.

[20] T. Steiner, *Angew. Chem. Int. Ed.* **2002**, *41*, 48-76.

[21] T. Kroon, J. A. Kanters, *Nature* **1974**, *248*, 667-669.

[22] E. Arunan, G. R. Desiraju, R. A. Klein, J. Sadlej, S. Scheiner, I. Alkorta, D. C. Clary, R. H. Crabtree, J. J. Dannenberg, P. Hobza, H. G. Kjaergaard, A. C. Legon, B. Mennucci, D. J. Nesbitt, *Pure Appl. Chem.* **2011**, *83*, 1637-1641.

[23] E. Dib, T. Mineva, E. Véron, V. Sarou-Kanian, F. Fayon, B. Alonso, *J. Phys. Chem. Lett.* **2018**, *9*, 19-24.

[24] E. Espinosa, E. Molins, C. Lecomte, *Chem. Phys. Lett.* **1998**, *285*, 170-173.

[25] X. Yang, *Mater. Res. Bull.* **2006**, *41*, 54-66.

[26] R. M. Shayib, N. C. George, R. Seshadri, A. W. Burton, S. I. Zones, B. F. Chmelka, *J. Am. Chem. Soc.* **2011**, *133*, 18728-18741.

[27] A. Corma, M. Puche, F. Rey, G. Sankar, S. J. Teat, *Angew. Chem. Int. Ed.* **2003**, *42*, 1156-1159.

[28] M. A. Camblor, M.-J. Díaz-Cabañas, J. Perez-Pariente, S. J. Teat, W. Clegg, I. J. Shannon, P. Lightfoot, P. A. Wright, R. E. Morris, *Angew. Chem. Int. Ed.* **1998**, *37*, 2122-2126.

[29] P. A. Barrett, M. A. Camblor, A. Corma, R. H. Jones, L. A. Villaescusa, *J. Phys. Chem. B* **1998**, *102*, 4147-4155.

[30] a) S. L. Burkett, M. E. Davis, *Chem. Mater.* **1995**, *7*, 920-928; b) C. S. Cundy, P. A. Cox, *Microporous Mesoporous Mater.* **2005**, *82*, 1-78; c) M. Moliner, F. Rey, A. Corma, *Angew. Chem. Int. Ed.* **2013**, *52*, 13880-13889; d) L. Gómez-Hortigüela, M. A. Camblor, in *Insights into the Chemistry of Organic Structure-Directing Agents in the Synthesis of Zeolitic Materials. Structure and Bonding 175* (Eds.: L. Gómez-Hortigüela, M. A. Camblor), Springer, Cham, **2018**, pp. 1-41.